

## Enhancing the accuracy of low-cost thermocouple devices through deep-wavelet neural network calibration

James Julian<sup>1</sup>, Fitri Wahyuni<sup>1</sup>, Annastya Bagas Dewantara<sup>2</sup>, Adi Winarta<sup>3</sup>, Nandy Putra<sup>4</sup>

<sup>1</sup>Department of Mechanical Engineering, Faculty of Engineering, University of Pembangunan Nasional Veteran Jakarta, Jakarta, Indonesia

<sup>2</sup>Department of Electrical Engineering, Faculty of Engineering, University of Pembangunan Nasional Veteran Jakarta, Jakarta, Indonesia

<sup>3</sup>Department of Mechanical Engineering, Politeknik Negeri Bali, Jimbaran Badung, Bali, Indonesia

<sup>4</sup>Applied Heat Transfer Research Group, Department of Mechanical Engineering, Universitas Indonesia, Depok, Indonesia

### Article Info

#### Article history:

Received Aug 8, 2023

Revised Feb 19, 2024

Accepted Feb 20, 2024

#### Keywords:

Calibration

Deep learning

Thermocouple sensor

VisuShrink

Wavelet transform

### ABSTRACT

Data collection using thermocouple sensors in low-cost data acquisition is prone to noise interference, which could reduce the data quality. Noise sources such as cold junction compensators, electromagnetic interference, and Johnson noise can significantly affect the reliability and accuracy of conventional measurements. This study aims to improve the quality of thermocouple sensor readings on low-cost data acquisition using calibration method based on deep learning and the denoising process using a wavelet transform. This taken approach successfully increase the accuracy value of 97.67% with a mean absolute error (MAE) of 0.2. The precision also increases of 262.7% as indicated by the result of signal-to-noise ratio (SNR) with a value of 105.29 dB. Comparative analysis was carried out against National Instruments® device and it was found that deep-wavelet method had a lower and higher of MAE and SNR<sub>dB</sub> values of 16.67% and 0.8% respectively. This study shows that the denoising-calibration method with deep-wavelet can improve the accuracy and reliability of data from low-cost thermocouple devices.

This is an open access article under the [CC BY-SA](https://creativecommons.org/licenses/by-sa/4.0/) license.



### Corresponding Author:

Adi Winarta

Department of Mechanical Engineering, Politeknik Negeri Bali

Politeknik Negeri Bali Campus, Bukit Jimbaran, South Kuta, Badung Bali 80361, Indonesia

Email: adi.winarta@pnb.ac.id

## 1. INTRODUCTION

Temperature is a fundamental parameter in sciences which influences many aspects of life particularly in thermal process. The wide use of these parameters has led to an increasing demand for accurate temperature measurement instruments. The global market data estimates that the annual growth of temperature sensors will increase by 4.8% in 2027 [1], and it is also predicted that in the next ten years will exceed 10 billion sensors/year [2]. The impact caused by this increased demand is the rise of the thermocouple modules price with high accuracy. Thus, the increasing demand of using of cheap sensors with low-quality accuracy will slowly increases. The level of accuracy and range of the temperature sensor is influenced by the type of sensor. Thermocouple, one of them, is widely used because of their broad range capability and quick response compare with others temperature sensor. Thermocouples also have more reasonable prices and easy handling compared with resistance temperature detectors (RTD), which is another type of temperature sensor [3]. The main problem found in thermocouple sensors is the presence of Johnson noise which is created due to thermal gradients at the reference junctions [4] caused by poor insulation, shielding, and temperature stabilization in

thermocouple data acquisition devices. Other noise created due to electromagnetic interference in electronic circuits and unstable input voltages due to ripple or poor grounding affects the quality of the readings output [5].

There are several approaches in minimizing the presence of noise in thermocouple sensor, one of them is applying the Kalman filter algorithm [6]. In fact, the process of implementing the Kalman filter is strongly depend on the system dynamic model which is set at the beginning and ineffective with the high variation data [7]. Another approach by Leon-Medina *et al.* [8] using a deep neural network has also been carried out to minimize the amount of noise contained in the thermocouple data and obtain the best of root mean squared error (RMSE) value of 1.19 °C. However, the presence of noise is still visible in the peak signal area. Yilmaz *et al.* [9] using fast Fourier transform (FFT) for denoising process, which is based on the observed frequency values. This method still has limitations in dealing with transient noise and frequency leakage, which are common in non-stationary signals such as sensor data readings. Papaioannou *et al.* [10] using moving average filter (MAF) to minimize errors in thermocouple sensor during temperature measurement in internal combustion engines with a maximum error value of 1.5% to 2% of peak temperature. The MAF filtering process has limitations in multiresolution analysis because it treats all component frequencies evenly. This method also does not respond well to non-stationary signals.

High fluctuation and noise generated by the thermocouple sensor cause conventional data acquisition techniques to be inaccurate and unreliable. The aim of our study was to examine the calibration and denoising method to improve the readings accuracy and quality of low-cost thermocouple device (DAQ) in order to overcoming the previous problems. This work contributes to understanding calibration techniques, guiding informed decisions in selecting appropriate temperature measurement methods for real-world applications.

## 2. METHOD

The calibration process was carried out using deep neural network on each thermocouple to reduce deviation values created to differences in the characteristics of each sensor. The denoising method also performed to reduce the uncertainty value which was created by interferences and Johnson noise. This method using wavelet transform by applying a threshold to each wavelet coefficient by entering the deviation value from each level. Both techniques are performed based on computer modeling by identifying the mean absolute error (MAE) value and signal-to-noise ratio (SNR) performance of the deep wavelet method.

This study begins with a calibration process of thermocouple sensors using Huber® controlled thermostatic bath (CTB) with high precision temperature controls ( $\pm 0.1$  °C). The process was performed to get the difference of temperature readings between the thermocouple and the actual temperature setup by the CTB. The temperature calibration ranging from 20 °C to 73 °C with a sampling frequency of 1 Hz for five minutes. Type-K of thermocouple was used in this experiment with length of 1,500 mm and a probe diameter of 3 mm. Some of the thermocouple was connected to the 32-channel of low-cost data acquisition (DAQ) module and the rest was connected to NI-9213 using NI-cDAQ 9174. Both of temperatures data were stored and analyze in one PC to avoid the inconsistency of elapsed time. Figure 1 shows the data collection process using two different DAQ (*e.g.* National Instrument® and low-cost thermocouple device/DAQ module). The artificial neural network (ANN) was then performed to calibrated the result data from the data collection process. The activation function of ANN architecture was varied so that enable of capturing complex pattern of the data. The smallest MAE of the activation function will be used by the ANN architecture for the denoising process using wavelet transform.

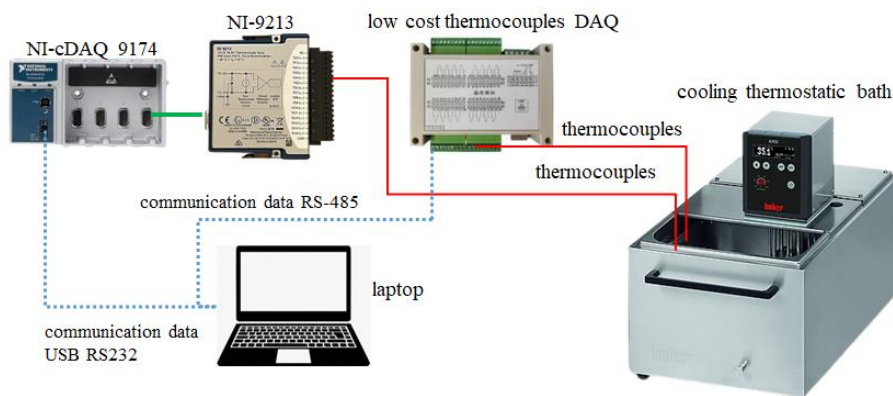


Figure 1. Schematic system of data collection setup

The reading data from both modules are analyzed using ANN and wavelet for its accuracy, precision, errors, and data fluctuations readings. Specifically, the deep-wavelet method's calibration and denoising capabilities were evaluated at temperatures ranging from 20 °C to 73 °C under steady-state conditions, considering each dataset's MAE, SNR<sub>dB</sub>, and uncertainty values. The MAE was used to analyze accuracy and systematic errors. Lower MAE values indicate a superior calibration. Additionally, signal-to-noise ratio in decibels (SNR<sub>dB</sub>) was employed to assess denoising performance. Higher values of SNR<sub>dB</sub> suggest effective noise reduction. Evaluating uncertainty provided valuable insights into the technique's reliability and robustness for low-cost thermocouple measurements with deep-wavelet. Ultimately, the comparison with NI-9213 and the application of deep-wavelet showed significant implications for enhancing temperature measurements' accuracy and reliability, particularly when employing low-cost thermocouples.

## 2.1. Artificial neural network

Artificial neural network (ANN) is a computational model system and created by mimicking the network pattern of the human brain so that it can recognize patterns and complex relationships in data [11]. The use of ANN in the calibration process using noisy data is suitable because of its ability to generalize and recognize outlier data [12]. ANN has an architecture consisting of layers of neurons with nodes connected. Interactions and relationships between each node in each layer have different weight and bias values which can function as regression or classification [13]. ANN performs learning through forward propagation to compute input values from data into initial node neurons to produce the expected output node. This process is performed through a computational process of adding weight and bias to each neuron node through a specific activation function [14]. The performance test of the ANN uses the MAE shown in (1) as the accuracy test performance of the regression model. This test is generally used due to intuitive interpretation of the model [15]. This MAE represents the accuracy of the data.

$$MAE = \frac{1}{N} \sum_{i=1}^N |a_j^l - \hat{y}_i| \quad (1)$$

N: Number of samples in batch data

The accuracy performance of the ANN model is affected by the given activation function [16]. During the calibration process, variations of the activation function are carried out by varying the activation function, namely rectified linear unit (ReLU), exponential linear unit (ELU), Gaussian error linear unit (GELU), linear and leaky ReLU. The choice of the ReLU activation function is due to its ability to deal with vanishing gradients [17]. ELU has ability to recognize noisy data and also used to prevent dying node neurons [18]. Linear is used to find out whether the simplification process can be used to ease model computation. GELU is used to overcome dying node neurons with lighter computation than ELU, and the asymptotic behavior of GELU provides a more stable training process [19]. Simplification of equations for computational process efficiency and prevention of dying node neurons is also found in Leaky ReLU [20] as stated in (2) to (6).

$$ReLU(z_j^l) = \begin{cases} 0 & \text{for } z_j^l < 0 \\ z_j^l & \text{for } z_j^l \geq 0 \end{cases} \quad (2)$$

$$ELU(z_j^l) = \begin{cases} \alpha \cdot (\exp(z_j^l) - 1), & \text{for } z_j^l < 0 \\ z_j^l & , \text{ for } z_j^l \geq 0 \end{cases} \quad (3)$$

$$GELU(z_j^l) = \frac{1}{2} \left( 1 + \operatorname{erf} \left( \frac{z_j^l}{\sqrt{2}} \right) \right) \quad (4)$$

$$Linear(z_j^l) = z_j^l \quad (5)$$

$$Leaky ReLU(z_j^l) = \begin{cases} \alpha \cdot z_j^l, & \text{for } z_j^l < 0 \\ z_j^l & , \text{ for } z_j^l \geq 0 \end{cases} \quad (6)$$

Backpropagation was used to optimize the weight and bias values of the model. Backpropagation performs optimization based on the error value obtained from the loss function equation with the actual and predicted values as input to the function [21]. The mean squared error (MSE) function is used rather than the mean absolute error (MAE) due to MSE performs well on data with a Gaussian distribution. MSE show in (9) not using a Laplacian distribution as a loss function distribution [22].

## 2.2. Wavelet transform

Wavelet transform is a mathematical technique for converting data from the time domain into the frequency domain and particularly used in processing and data analysis. For multiresolution analysis, time domain is easier to use than the Fourier transform, which only presents data in the form of the frequency domain [23]. Wavelet transform has more adaptability than Fourier transform in terms of noise suppression. This is because the threshold given to each coefficient is different at each level, which makes the use of Wavelet transform have various implementations [24]–[28].

Wavelet discrete transform is used because of its computational efficiency, which resembles fast Fourier transform. Discrete wavelet transform is more commonly used than continuous wavelet transforms for signal decomposition [29]. The Haar transformation is used in the noise reduction function because of its simplicity, versatility, and computational efficiency [30], as shown in (7) and (8).

$$\varphi[n] = \begin{cases} 1, & \text{if } 0 \leq n < \frac{N}{2} \\ -1, & \text{if } \frac{N}{2} \leq n < N \\ 0, & \text{otherwise} \end{cases} \quad (7)$$

$$\phi[n] = \begin{cases} 1, & \text{if } 0 \leq n < N \\ 0, & \text{otherwise} \end{cases} \quad (8)$$

where  $N$  is number of signal input;  $\varphi[n]$  is wavelet function at level- $j$  and position- $k$ ; and  $\phi[n]$  is wavelet scaling function at level- $j$  and position- $k$ .

In the thresholding process, the VisuShrink (10) is used because of its ability to overcome additive noise, which commonly occurs in sensors [31]. The deviation value for each level is calculated using (9) and (10) to determine global thresholding. The global thresholding value will be used for the denoising process for each wavelet coefficient. The SNR equation measures the wavelet transform's denoising performance against the equation's actual value (13). The uncertainty value is calculated using the mean deviation in (12) to find out the reliability data. All the equations are shown in (9)–(13):

$$M = J \times K \quad (9)$$

$$\hat{\sigma} = \frac{\text{median}(|cD_j|)}{0.6745} \quad (10)$$

$$\mu = \frac{1}{N} \sum_{n=0}^{N-1} x[n] \quad (11)$$

$$MAD = \frac{1}{N} \sum_{n=0}^{N-1} \left| x[n] - \left( \frac{1}{N} \sum_{n=0}^{N-1} x[n] \right) \right| \quad (12)$$

$$SNR_{dB} = 10 \log \left( \frac{\mu^2}{\sqrt{\frac{1}{N-1} \sum_{n=0}^{N-1} (x[n] - \mu)^2}} \right) \quad (13)$$

where  $\hat{\sigma}$  is signal deviation;  $K$  is number of coefficients at level- $j$ ;  $J$  is number of levels;  $T$  is universal thresholding;  $MAD$  is mean absolute deviation; and  $\mu$  is mean data.

## 3. RESULTS AND DISCUSSION

### 3.1. Data calibration

Figure 2 shows the data of thermocouple sensor from low-cost DAQ compare with actual temperature values from CTB settings within range from 20 °C to 73 °C. Data from low-cost DAQ shows different offset variations to the actual temperature set. The graph also shows the presence of evenly distributed noise related to the noise caused by the cold junction compensator in the amplifier contained in the thermocouple module [32]. The data shows that the magnitude of the noise fluctuation is different at low temperature and high temperatures, which might be caused by the presence of Johnson noise. This noise creates the current that flowing from sensor to thermocouple module fluctuates due to increase of thermal energy and vibrations from the water as a reading environment [33].

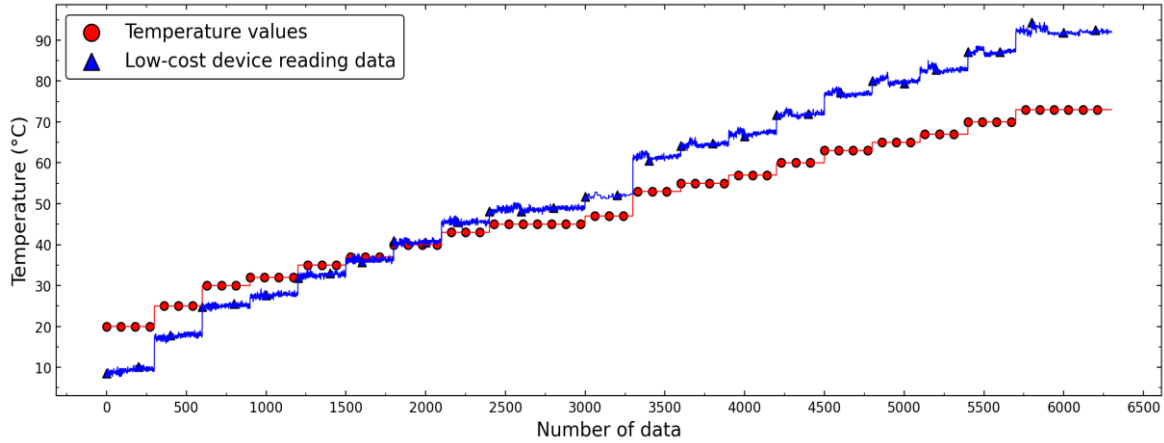


Figure 2. Calibration between thermocouple sensor readings and actual temperature data readings

Deep learning using ANN is performed to reduce noise by varying the type of activation function in (2) to (6). In this work two-layer architecture were used. Eight neuron nodes in the first layer and one neuron node in the second layer with both having the same type of activation. The training process was carried out with  $\alpha$  value of 0.001 and  $i$  of 1,000 iterations as shown in Figure 3. The ELU activation function has the lowest MAE value and GELU with a faster convergent time than the other four activation functions. In addition, ELU, has high results when trained on data with high noise. Our result in this stage shows linear consistency with Poulinakis *et al.* [34].

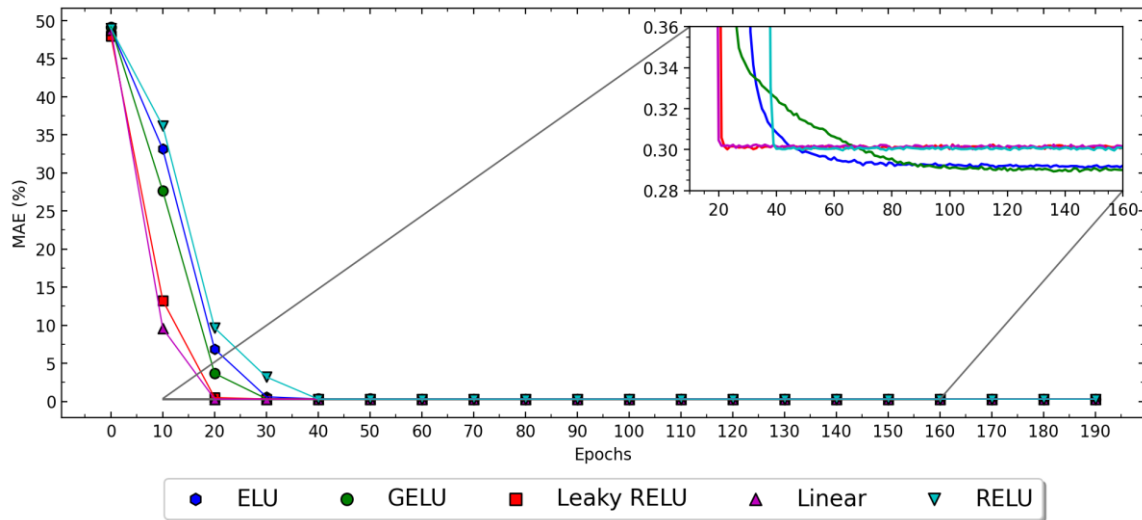


Figure 3. Activation functions MAE comparisons

**3.2. Denoising signal**

The next process is to carry out analysis using wavelet transform as a denoising process with a  $J$  level value of 6 and total  $N$  of 6,300. The decomposition results of the wavelet transform calculated using (7) to (10). Figure 4 shows the results of the wavelet decomposition process. The value of  $cA_{j,k}$  and  $cD_{j,k}$  represents the coefficient of the approximation. Detail coefficients at the  $j$ -level, the  $k$ -signal and  $cA_{j,k}^*$ ,  $cD_{j,k}^*$  represents the approximation and detail coefficients respectively, after denoising with wavelet transform. The results are indicating that the value  $cA_{6,k}$  shows the same trend as the input signal from deep learning calibration. This might be due to the value of  $cA_{6,k}$  represents values at low frequencies. In addition, the sampling frequency during the data collection process, which is 1 Hz, makes deep learning data emphasize the low-frequency trend in  $cA_{6,k}$ . In  $cD_{5,k}$  high frequencies caused by fluctuations begin to appear.

These fluctuations are caused by the presence of Johnson noise and other noise, which is created from cold junction compensators on low-cost devices. The denoising process can be seen in each of the coefficients of  $cA_{j,k}^*$  and  $cD_{j,k}^*$  especially at high frequency. The noise of  $cD_{6,k}^*$  can no longer be seen due to the influence of the denoising process.

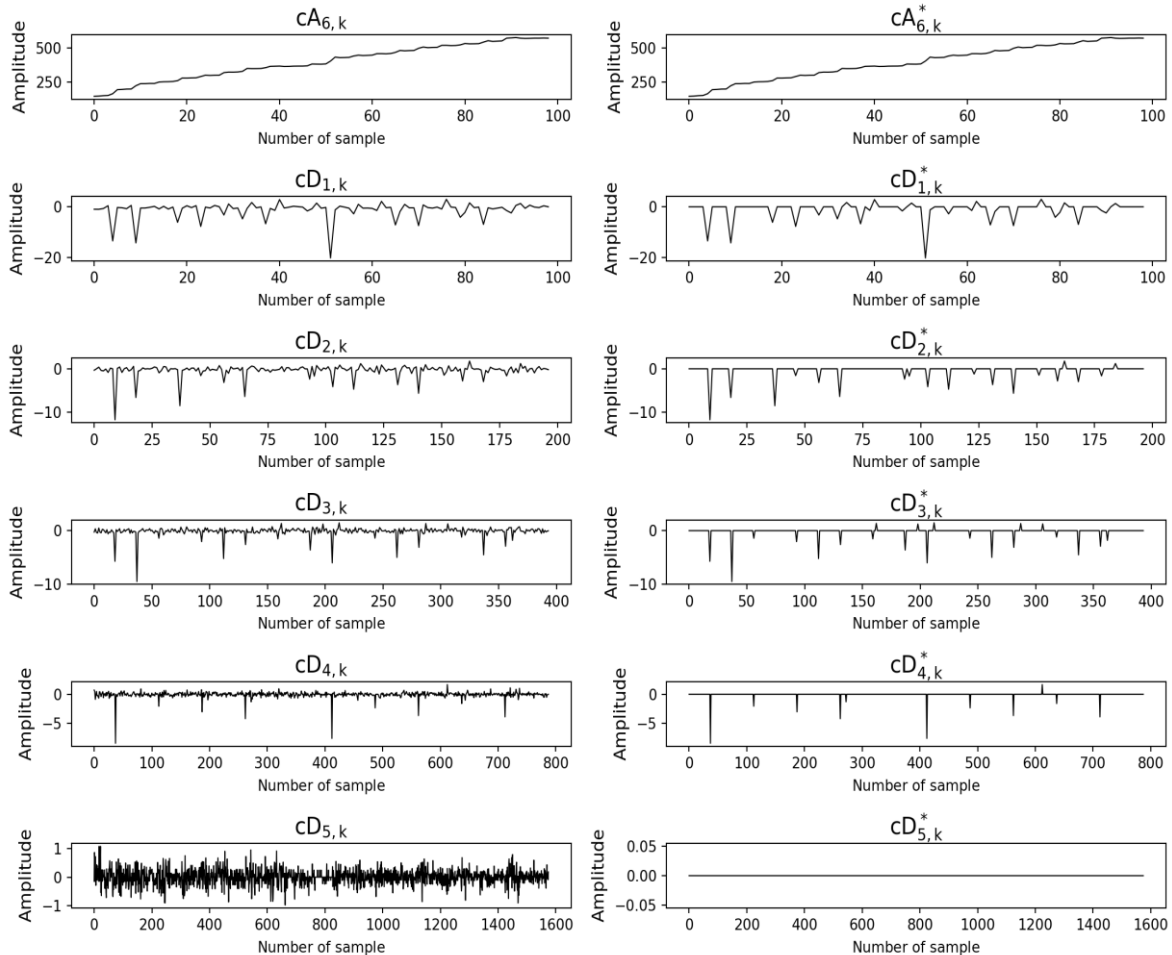


Figure 4. Deep-wavelet denoising process

Comparison of the initial measurements using low-cost DAQ, deep-wavelet, and NI-9213 was carried out using the error plot graph as shown in Figure 5. The average and deviation value of the total data collection in temperature varies from 20 °C to 73 °C. Based on our result, it is shown that the measurements made by the low-cost DAQ have good measurements in the range of 37 °C to 40 °C with an offset value that gets bigger with every increase in temperature.

Table 1 shows the performance calculation of each measurement from the low-cost DAQ, deep-wavelet and NI-9213. The average MAE from the deep-wavelet shows the lowest value compared with others. There is a reduction of MAE of 97.67% percent, which indicates a good performance of calibration. The average MAE value of deep-wavelet is lower than NI-9213 about 16.67%. The  $SNR_{dB}$  performance for deep-wavelet is also superior to low-cost DAQ with the increase of 262.7% and higher than NI-9213 about 0.8%. Noise reduction of 65.22 dB was achieved using deep-wavelet through a hard thresholding process with VisuShrink. This result on  $SNR_{dB}$  shows the denoising process works well in increasing data reliability. On the other hand, Table 1 also shows that uncertainty (e.g. mean deviation) of deep-wavelet analysis decreases about 60% from initial value. This uncertainty of deep-wavelet is still lower about 0.02 compared with NI-9213. This indicates that the method of increasing the accuracy using deep-wavelet have high robustness and reliability even though the hardware device were performed through a low-cost DAQ.

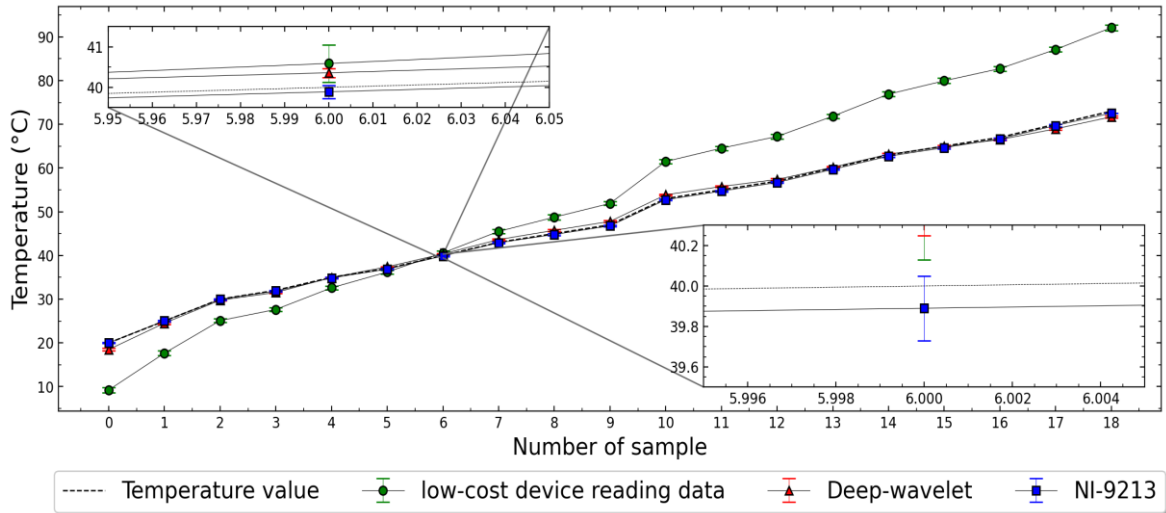


Figure 5. Deep-wavelet results

Table 1. Comparison of performances

Temperature value	MAE			SNR <sub>dB</sub>			Mean deviation		
	Low-cost DAQ	Deep-wavelet	NI-9213	Low-cost DAQ	Deep-wavelet	NI-9213	Low-cost DAQ	Deep-wavelet	NI-9213
Average	8.59	0.2	0.24	40.07	105.29	104.45	0.4	0.16	0.14

#### 4. CONCLUSION

This study investigated the improvement methods of temperature reading from a low-cost DAQ for thermocouples sensors using deep-wavelet method. The performance evaluation used MAE, SNR<sub>dB</sub>, and measurement uncertainty. The results demonstrated a significant advantage of the deep-wavelet with an average MAE value of 0.2. An increase in accuracy of 97.67% from the low-cost measurement shows the success of the calibration process from deep-wavelet as a superior calibration method for accurate temperature estimation. The denoising process based on deep-wavelet is known to increase the reliability of temperature data, with an increase in SNR<sub>dB</sub> of 262.7% from the low-cost device. Comparative analysis of Deep-wavelet performance against NI-9213 shows an advantage of 0.84 dB in noise reduction through a hard thresholding process with VisuShrink. Although the NI-9213 exhibits the lowest uncertainty level about 0.14 the mean deviation of Deep wavelet method still shows a good achievement, which is only differ about 0.02. This research demonstrates the potential of deep-wavelet method as an efficient solution for improving the accuracy of low-cost DAQ which is susceptible to noise effects.

#### REFERENCES

- [1] A. Elyounsi and A. N. Kalashnikov, "Evaluating suitability of a DS18B20 temperature sensor for use in an accurate air temperature distribution measurement network," in *Engineering Proceedings*, Nov. 2021, vol. 10, no. 1, doi: 10.3390/ecs-a-11277.
- [2] R. Bogue, "Towards the trillion sensors market," *Sensor Review*, vol. 34, no. 2, pp. 137–142, Mar. 2014, doi: 10.1108/SR-12-2013-755.
- [3] M. Pandey and G. Mishra, "Types of sensor and their applications, advantages, and disadvantages," in *Advances in Intelligent Systems and Computing*, vol. 814, Springer Singapore, 2019, pp. 791–804.
- [4] J. F. Qu, S. P. Benz, H. Rogalla, W. L. Tew, D. R. White, and K. L. Zhou, "Johnson noise thermometry," *Measurement Science and Technology*, vol. 30, no. 11, p. 112001, Sep. 2019, doi: 10.1088/1361-6501/ab3526.
- [5] S. B. Barnett, A. G. Swanson, T. Lorimer, and M. Brown, "Electromagnetic interference mitigation in a high voltage inspection robot," in *Lecture Notes in Electrical Engineering*, vol. 598 LNEE, Springer International Publishing, 2020, pp. 331–341.
- [6] R. Septiana, I. Roihan, and R. A. Koestoer, "Denoising MAX6675 reading using Kalman filter and factorial design," *International Journal of Electrical and Computer Engineering*, vol. 11, no. 5, pp. 3818–3827, Oct. 2021, doi: 10.11591/ijece.v11i5.pp3818-3827.
- [7] C. Urrea and R. Agramonte, "Kalman filter: Historical overview and review of its use in robotics 60 years after its creation," *Journal of Sensors*, vol. 2021, pp. 1–21, Sep. 2021, doi: 10.1155/2021/9674015.
- [8] J. X. Leon-Medina *et al.*, "Temperature prediction using multivariate time series deep learning in the lining of an electric arc furnace for ferronickel production," *Sensors*, vol. 21, no. 20, Art. no. 6894, Oct. 2021, doi: 10.3390/s21206894.
- [9] N. Yilmaz, W. Gill, A. B. Donaldson, and R. E. Lucero, "Problems encountered in fluctuating flame temperature measurements by thermocouple," *Sensors*, vol. 8, no. 12, pp. 7882–7893, Dec. 2008, doi: 10.3390/s8127882.

- [10] N. Papaioannou, F. Leach, and M. Davy, "Effect of thermocouple size on the measurement of exhaust gas temperature in internal combustion engines," in *SAE Technical Papers*, Sep. 2018, vol. 2018-Sept, doi: 10.4271/2018-01-1765.
- [11] E. Grossi and M. Buscema, "Introduction to artificial neural networks," *European Journal of Gastroenterology and Hepatology*, vol. 19, no. 12, pp. 1046–1054, Dec. 2007, doi: 10.1097/MEG.0b013e3282f198a0.
- [12] A. E. Ilesanmi and T. O. Ilesanmi, "Methods for image denoising using convolutional neural network: a review," *Complex and Intelligent Systems*, vol. 7, no. 5, pp. 2179–2198, Jun. 2021, doi: 10.1007/s40747-021-00428-4.
- [13] N. Yuvaraj, R. A. Raja, N. V. Kousik, P. Johri, and M. J. Diván, "Analysis on the prediction of central line-associated bloodstream infections (CLABSI) using deep neural network classification," in *Computational Intelligence and Its Applications in Healthcare*, Elsevier, 2020, pp. 229–244.
- [14] O. A. Montesinos López, A. Montesinos López, and J. Crossa, "Fundamentals of artificial neural networks and deep learning," in *Multivariate Statistical Machine Learning Methods for Genomic Prediction*, Springer International Publishing, 2022, pp. 379–425.
- [15] A. de Myttenaere, B. Golden, B. Le Grand, and F. Rossi, "Mean absolute percentage error for regression models," *Neurocomputing*, vol. 192, pp. 38–48, Jun. 2016, doi: 10.1016/j.neucom.2015.12.114.
- [16] K. Biswas, S. Kumar, S. Banerjee, and A. K. Pandey, "EIS - Efficient and trainable activation functions for better accuracy and performance," in *Lecture Notes in Computer Science (including subseries Lecture Notes in Artificial Intelligence and Lecture Notes in Bioinformatics)*, vol. 12892 LNCS, Springer International Publishing, 2021, pp. 260–272.
- [17] A. Nguyen, K. Pham, D. Ngo, T. Ngo, and L. Pham, "An analysis of state-of-the-art activation functions for supervised deep neural network," in *Proceedings of 2021 International Conference on System Science and Engineering, ICSSSE 2021*, Aug. 2021, pp. 215–220, doi: 10.1109/ICSSSE52999.2021.9538437.
- [18] D. A. Clevert, T. Unterthiner, and S. Hochreiter, "Fast and accurate deep network learning by exponential linear units (ELUs)," *4th International Conference on Learning Representations, ICLR 2016 - Conference Track Proceedings*, Nov. 2016.
- [19] D. Hendrycks and K. Gimpel, "Gaussian error linear units (GELUs)," *Arxiv.org/abs/1606.08415*, Jun. 2016.
- [20] B. Xu, N. Wang, T. Chen, and M. Li, "Empirical evaluation of rectified activations in convolutional network," *arxiv.org/abs/1505.00853*, May 2015.
- [21] J. C. R. Whittington and R. Bogacz, "Theories of error back-propagation in the Brain," *Trends in Cognitive Sciences*, vol. 23, no. 3, pp. 235–250, Mar. 2019, doi: 10.1016/j.tics.2018.12.005.
- [22] T. O. Hodson, "Root-mean-square error (RMSE) or mean absolute error (MAE): when to use them or not," *Geoscientific Model Development*, vol. 15, no. 14, pp. 5481–5487, Jul. 2022, doi: 10.5194/gmd-15-5481-2022.
- [23] S. A. P. Haddad and W. A. Serdijn, "Wavelet versus Fourier Analysis," in *Ultra Low-Power Biomedical Signal Processing*, Springer Netherlands, 2009, pp. 33–50.
- [24] L. Ramalingappa and A. Manjunatha, "Power quality event classification using complex wavelets phasor models and customized convolution neural network," *International Journal of Electrical and Computer Engineering*, vol. 12, no. 1, pp. 22–31, Feb. 2022, doi: 10.11591/ijece.v12i1.pp22-31.
- [25] A. B. Channegowda and H. N. Prakash, "Image fusion by discrete wavelet transform for multimodal biometric recognition," *IAES International Journal of Artificial Intelligence*, vol. 11, no. 1, pp. 229–237, Mar. 2022, doi: 10.11591/ijai.v11.i1.pp229-237.
- [26] M. Hamiane and F. Saeed, "SVM classification of MRI brain images for computer-assisted diagnosis," *International Journal of Electrical and Computer Engineering (IJECE)*, vol. 7, no. 5, pp. 2555–2564, Oct. 2017, doi: 10.11591/ijece.v7i5.pp2555-2564.
- [27] J. Too, A. R. Abdullah, N. M. Saad, N. M. Ali, and H. Musa, "A detail study of wavelet families for EMG pattern recognition," *International Journal of Electrical and Computer Engineering (IJECE)*, vol. 8, no. 6, pp. 4221–4229, Dec. 2018, doi: 10.11591/ijece.v8i6.pp4221-4229.
- [28] Lakshmikanth S, K. R. Natraj, K. R. Rekha, "Noise and vibration reduction In PMSM –A review," *International Journal of Electrical and Computer Engineering (IJECE)*, vol. 2, no. 3, pp. 405–416, Apr. 2012, doi: 10.11591/ijece.v2i3.322.
- [29] S. M. Alessio, "Discrete wavelet transform (DWT)," in *Digital Signal Processing and Spectral Analysis for Scientists*, Springer International Publishing, 2016, pp. 645–714.
- [30] J. Bhardwaj and A. Nayak, "Haar wavelet transform-based optimal Bayesian method for medical image fusion," *Medical and Biological Engineering and Computing*, vol. 58, no. 10, pp. 2397–2411, Jul. 2020, doi: 10.1007/s11517-020-02209-6.
- [31] S. Ruikar and D. D. Doye, "Image denoising using wavelet transform," in *ICMET 2010 - 2010 International Conference on Mechanical and Electrical Technology, Proceedings*, Sep. 2010, pp. 509–515, doi: 10.1109/ICMET.2010.5598411.
- [32] B. Balko and R. L. Berger, "Measurement and computation of thermojunction response times in the submillisecond range," *Review of Scientific Instruments*, vol. 39, no. 4, pp. 498–503, Apr. 1968, doi: 10.1063/1.1683416.
- [33] D. R. White *et al.*, "The status of Johnson noise thermometry," *Metrologia*, vol. 33, no. 4, pp. 325–335, Aug. 1996, doi: 10.1088/0026-1394/33/4/6.
- [34] K. Poulinakis, D. Drikakis, I. W. Kokkinakis, and S. M. Spottswood, "Machine-learning methods on noisy and sparse data," *Mathematics*, vol. 11, no. 1, Art. no. 236, Jan. 2023, doi: 10.3390/math11010236.

## BIOGRAPHIES OF AUTHORS



**James Julian**    was born in Jakarta on July 18<sup>th</sup>, 1986. He received his bachelor's degree in mechanical engineering from Universitas Pancasila in 2012 and obtained his master's degree from Universitas Indonesia in 2015. Furthermore, he received his Doctor of Engineering degree also from Universitas Indonesia. Currently he serves as lecture in Department of Mechanical Engineering, Universitas Pembangunan Nasional Veteran Jakarta (UPNVJ), Indonesia. His research is currently focused on fluid mechanics, machine learning and especially on the application of a plasma actuator on flow control. He is also interested in the application of computational fluid dynamics. He can be contacted at email: zames@upnvj.ac.id.



**Annastya Bagas Dewantara**    received the bachelor's degree in electrical engineering from the University Pembangunan Nasional Veteran Jakarta, Jakarta, Indonesian, was born in Jakarta on December 08<sup>th</sup>, 2001. His field includes electronics, microcontrollers, and control system. He is also interested in embedded system, IoT and sensor network. He can be contacted at email: [annastya.bd@upnvj.ac.id](mailto:annastya.bd@upnvj.ac.id).



**Fitri Wahyuni**    was born in Bukit Tinggi on July 2<sup>nd</sup>, 1985. She completed her Bachelor of Physics education at the Jakarta State University in 2009 and her master's in mechanical engineering at Gadjah Mada University in 2013. From 2014 to 2019 she worked as a lecturer in Industrial Engineering, Indraprasta University, PGRI. From 2019 until now he has worked as a Lecturer in mechanical engineering at the Veterans National Development University in Jakarta. At present, the area of research that is being developed is construction machinery. She can be contacted at email: [fitriwahyuni@upnvj.ac.id](mailto:fitriwahyuni@upnvj.ac.id).



**Adi Winarta**    was born in Singaraja, Bali on October 10<sup>th</sup>, 1976. He received his bachelor's degree in mechanical engineering from Institut Teknologi Nasional (ITN) in 2001. In 2018, he received his Doctor of Mechanical Engineering degree from the University of Indonesia. His research is currently focused on pulsating heat pipes, thermoelectric, phase change material, refrigeration, and air conditioning. He is also interested in instrumentation and control, especially in building automation control systems for commercial HVAC buildings. He can be contacted at email: [adi.winarta@pnb.ac.id](mailto:adi.winarta@pnb.ac.id).



**Nandy Putra**    born in Palembang on October 25<sup>th</sup>, 1970, the esteemed professor is a prominent figure at the University of Indonesia. He earns his bachelor's degree in mechanical engineering in 1994 in University of Indonesia with the project of Aero flit design and testing. He is a doctoral graduate in heat transfer from Universität der Bundeswehr Hamburg in 2002. Working as lecturer in mechanical engineering and granted a professor title in 2009. His instructional spectrum spans heat transfer, mechanical design, energy conversion machines, and more. He created Applied Heat Transfer Research Group (AHTRG) at the Faculty of Engineering, University of Indonesia, nurturing and supporting many of his students to work in research in the fields of heat pipes, nanofluids, and phase change materials. He can be contacted at email: [nandyputra@eng.ui.ac.id](mailto:nandyputra@eng.ui.ac.id).